



THz generation by optical rectification of femtosecond laser pulses in a liquid crystal

LEI WANG,^{1,2,†} HONGSONG QIU,^{3,†} PING JIN,² SHIJUN GE,¹ ZHIXIONG SHEN,¹ WEI HU,¹  BINGXIANG LI,²  MAKOTO NAKAJIMA,⁴ BIAOBING JIN,³ AND YANQING LU^{1,*}

¹College of Engineering and Applied Sciences, Key Laboratory of Intelligent Optical Sensing and Manipulation, Nanjing University, Nanjing 210093, China

²College of Electronic and Optical Engineering & College of Microelectronics, Nanjing University of Posts and Telecommunications, Nanjing 210023, China

³Research Institute of Superconductor Electronics (RISE), School of Electronic Science and Engineering, Nanjing University, Nanjing 210093, China

⁴Institute of Laser Engineering, Osaka University, Suita, Osaka 565-0871, Japan

*Corresponding author: yqlu@nju.edu.cn

Received 11 October 2021; revised 14 December 2021; accepted 22 December 2021; posted 22 December 2021; published 25 February 2022

In this study, we propose the generation of broadband terahertz (THz) radiation from a liquid crystal with large birefringence in the THz range, pumped by 800 nm femtosecond laser pulses based on optical rectification. Our measurements revealed that the THz amplitude depends on the orientation of the liquid crystal relative to the polarization of the femtosecond pump. Additionally, it was found that the THz peak intensity is linearly dependent on the pump fluence. Furthermore, an elliptically polarized THz wave pattern was observed. The results may lead to a new type of tunable THz source. © 2022 Optica Publishing Group

<https://doi.org/10.1364/JOSAB.445568>

1. INTRODUCTION

Electromagnetic radiation in the terahertz (THz) frequency range, from 0.1–10 THz, plays a significant role in various domains, such as material spectroscopy, nondestructive evaluation, biomedical diagnosis, and high-speed wireless communication [1–3]. However, the requirements of power, bandwidth, and polarization for THz radiation, especially flexible, tunable, and easy to use, are urgent for improving the performance of THz applications. With the development of ultrafast lasers, various types of THz sources with broadband are being developed. THz waves can be emitted from GaAs photoconductive antennas [4]. Gases, such as air [5], and liquids, such as water [6], can generate THz pulse radiation. Additionally, THz emissions have been reported from ferromagnet/heavy-metal and antiferromagnet/heavy-metal structures [7,8]; however, it is difficult to control the polarization of these THz emissions. A 3D topological insulator has realized the generation and manipulation of chiral THz waves [9].

Optical rectification (OR) is a mechanism commonly used to produce broadband and powerful THz pulses. The generation scheme is relatively simple. Various types of THz sources based on OR progress rapidly. The applicable materials include semiconductor, organic, and inorganic crystals. In 2007, 1.5 μ J single-cycle THz pulses were generated from a large aperture

ZnTe crystal [10]. Organic crystals usually have larger second-order nonlinear susceptibilities and higher conversion efficiency, and can produce a wider THz spectrum than inorganic crystals. As early as in 1992, Prof. Zhang reported THz OR from a nonlinear organic crystal, dimethyl amino 4-N-methylstilbazolium tosylate (DAST), with optical excitation at a wavelength and pulse duration of 820 nm and 150 fs, respectively [11]. Recently, Buchmann *et al.* demonstrated the first MHz-repetition-rate, broadband THz source based on OR in organic crystals, 2-(4-hydroxy-3-methoxystyryl)-1-methylquinolinium 2,4,6-trimethylbenzenesulfonate (HMQ-TMS), driven at 1035 nm with a pulse duration of 30 fs [12]. However, phonon absorptions are present in the THz band in organic crystals, and the resultant THz spectrum is complex [13]. OR in lithium niobate (LN) is suitable for obtaining high-power THz radiation owing to its large effective nonlinearity and high damage threshold. However, its refractive index in the optical band differs significantly from that in the THz band. The pulse front of the pump laser must be tilted to achieve phase matching over significant propagation lengths, thus increasing complexity [14,15]. THz generation based on the OR effect is generally linearly polarized; thus, elliptically or circularly polarized THz waves still remain a challenge.

Solids, liquids, and gases can produce THz wave radiation based on femtosecond lasers. However, THz generation from liquid crystals (LCs), which are between the solid and liquid phase, has not yet been reported. LCs, which are widely used

is display devices, uniquely combine the anisotropy from the long-range order of solid crystals with the fluidity of fluid phases [16]. Their director (average molecular orientation) and optical property depend on surface alignment, and they are sensitive to external fields [17]. The photo-alignment technique can be used to precisely control the director distribution of LCs [18–20]. The centrosymmetry possessed by almost all LCs can be broken optically [21]; moreover, their special nonlinear optical properties can trigger interesting effects, such as fast all-optical switching [22]. The second-order nonlinear response of LCs is approximately five times larger in the ordered phase than that in the isotropic (disordered) phase [23]. It is worth studying whether the interactions between femtosecond lasers and LCs can produce THz radiation. In this work, we demonstrate broadband THz radiation in a type of LC pumped by a femtosecond laser owing to its relatively large second-order nonlinearity and small THz absorption, and observe the changes in the polarization of THz waves.

2. METHODOLOGY

The schematic of the THz emission spectroscopy setup is illustrated in Fig. 1, with the coordinate system (xyz) defined for the laboratory frame. A Ti:sapphire femtosecond amplifier with a central wavelength, pulse width and repetition rate of 800 nm, ~ 100 fs, and 1 kHz, respectively, was used as the pump. The pump was propagated along the z axis with linear polarization parallel to the y axis. The y component of the generated THz electric field was measured in the time domain through electro-optical sampling. The LC cell was arranged perpendicular to the z axis. It was composed of two parallel fused silica substrates separated by approximately 180 μm mylar films to control the cell gap. Both substrates were spin coated with sulfonic azo dye as an alignment layer and photo-aligned to achieve homogeneous pre-alignment at 45° to the y axis. A nematic LC NJU-LDn-4 with high birefringence (approximately 0.3) in the THz range was filled into the gap; its absorption was relatively small, which was beneficial for THz emission [24]. The director of the LC was initially at an angle of 45° to the y axis. The angle between the director and polarization of the optical pump beam is indicated by θ . The pump beam was loosely focused on the LC cell with a spot diameter of around 2 mm. Based on the same mechanism, i.e., the OR effect, as other crystals generating THz radiation, when the intense optical pulses with a broad spectrum are incident to the LC, the nonlinear interaction between any two frequency components within the spectrum induces dielectric polarization and radiates broadband electromagnetic waves at the THz frequency.

3. RESULTS AND DISCUSSION

First, the influence of the relative direction between the pump polarization and LC orientation on THz radiation was investigated because crystal orientation is generally related to THz production efficiency. As shown in Fig. 2(a), at the initial position, when the LC director is at an angle of 45° to pump polarization, the produced THz pulse is demonstrated as shown by the black curve. Then, the LC cell is rotated by 45° such that the director of LC is parallel to pump polarization ($\theta = 0^\circ$),

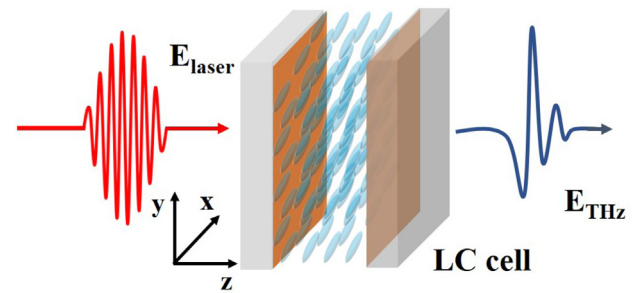


Fig. 1. Schematic of the THz emission spectroscopy setup. E_{laser} and E_{THz} represent the electric fields of the pump laser and THz emission, respectively. The pump laser propagates along the z axis with the polarization parallel to the y axis.

thereby resulting in a larger THz signal and delay with respect to the signal when $\theta = 45^\circ$. When the LC director is perpendicular to pump polarization ($\theta = 90^\circ$), almost no THz radiation is detected; it may be too small to be detected. Here, the power of the pump beam is 30 mW. The corresponding THz frequency spectra are demonstrated in Fig. 2(b). The generated broadband THz radiation exhibits a spectral peak around 1.2 THz. The generated frequency spectrum is greater when the LC director is parallel to the polarization of the incident optical pump. The observed differences in spectra could be attributed to the differences in the influence of the fs-laser induced director reorientation on the second-order nonlinear susceptibility of the LC and phase matching. To maximize THz generation efficiency, it should be ensured that the LC director is along the surface plane of the LC cell and parallel to the polarization of the incident pump beam [25]. The dependence of the radiated THz electric field on LC orientation can be attributed to the LC orientation dependence of the induced polarization at the beat frequency. The angular-dependent results provide evidence that second-order OR is the major nonlinear process for THz emission under the condition of moderate optical fluence and normal incidence on the LC. To obtain a general rule, we selected the general case (θ is approximately 45°) to analyze in the following study.

Pump excitation-dependent THz radiation was studied. The pump beam with different powers is incident on the LC cell, and the generated THz time domain waveforms are shown in Fig. 3(a). When the pump power is 10 mW, the generated THz wave is too weak and can barely be observed. When the pump power is increased to 15 mW, an obvious THz signal appears. The intensity of the THz pulse increases with the pump power. However, the THz time-domain spectra are nearly the same when the pump power is 30 and 35 mW. The measured time-domain THz waveforms are almost identical because the characteristics of THz radiation are determined by the pump wavelength, pulse width, crystal thickness, and orientation [26]. Figure 3(b) shows the THz peak electric field and energy from LC as a function of the pump fluence; it can be observed that the relationship between the absolute values of the measured THz peak amplitude and laser fluence is linear. Moreover, a quadratic relationship is demonstrated between the THz energy and laser fluence. The dependence of THz emission from the LC on pump power is the same as that from other crystal materials based on the OR effect, which can be described as follows [27]:

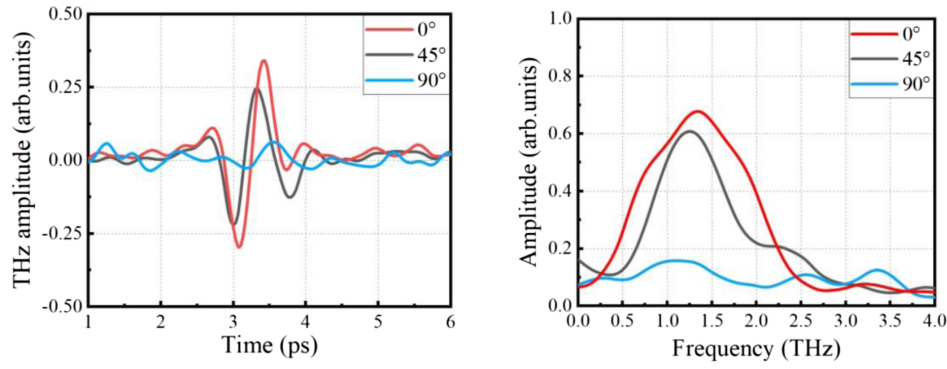


Fig. 2. (a) Temporal THz waveforms of the THz emission from the LC cell with different θ . (b) Corresponding Fourier-transformed spectra.

$$E_{\text{THz}} \propto \frac{\partial^2 P(t)}{\partial t^2} = \chi^{(2)} \frac{\partial^2 E_{\text{laser}}^2(t)}{\partial t^2}, \quad (1)$$

where $\chi^{(2)}$ denotes the second-order susceptibility, which depends on the crystal structure of the material. E_{laser} is the electric field of the pump pulse. The amplitude of the radiated THz electric field from the LC is proportional to the second time derivative of the optically induced dielectric polarization, which further proves that THz generation from LCs is based on the OR of femtosecond laser pulses. Figure 3(b) shows that the laser excitation pulse energy threshold for the detectable THz field from the LC is approximately 0.2 mJ/cm². The THz amplitude was found to be saturated at 0.15 V/cm. The damage threshold of the LC is approximately 1.2 mJ/cm²; it breaks when the energy of the excitation pulse is over 1.2 mJ/cm². The dotted parts of the curves deviate from the tendency. We think that in the low pump fluence region, noise has much influence, while in the high region, free carriers generated by two-photon absorption [28] as well as the low damage threshold of the LC may explain the saturation of THz radiation. In contrast, common LC materials with the same cell structure, such as E7, do not exhibit THz radiation even for 35 mW laser pumps. Moreover, the fused silica substrates of the LC cell and the same empty cell demonstrate no THz emission.

Next, the different polarization states of the THz frequencies can be observed using two combined wire grid polarizers. The propagation direction is set to 45° and −45° with respect to the y axis for the front wire grid and fixed parallel to the y axis for the rear one. Figure 4(a) shows the three-dimensional trajectory plot of the temporal waveforms of THz emission. It is evident

that THz radiation is not linearly polarized. We extracted the phase difference between the 45° and −45° components using Fourier transform on the experimental data, plotted in Fig. 4(b). It can be observed that the left-handed elliptically polarized THz waves were generated at different THz frequencies. We compared the results with those obtained by ZnTe, in which the THz radiation was linearly polarized with no phase difference.

The evident ellipticity is the main characteristic from our LC OR process. It is probable that LC reorientation is induced by the femtosecond laser pump, leading to nonuniform global orientation [29]. The centrosymmetry possessed by almost all LCs was broken by the planar orientation and optical pump. The absence of an effective center of symmetry indeed resulted in LC second-order nonlinear susceptibility. Our LC materials NJU-LDn-4 contain highly conjugated rod-like molecules, which are preferred to achieve relatively large nonlinearity, while E7 is not; moreover, they exhibited low absorption loss and no absorption peak in the THz range. Thus, they can be used for THz emission. So, it is reasonable that no THz radiation from E7 under the same experimental condition is detected. E7 may generate THz emission under other conditions. Here, we focus on THz generation from our LC NJU-LDn-4 first. We also have a spectrum similar to Fig. 2. in Ref. [29]; however, our second-harmonic generation (SHG) may be drowned in the luminescence (fluorescence), and it is difficult for us to distinguish them. We believe that SHG generated in LC can be proved by the detected THz radiation. The relationship between SHG and THz is complicated in LCs, compared with common crystals based on OR because of fs laser-induced director reorientation of LCs. The damage threshold of LCs

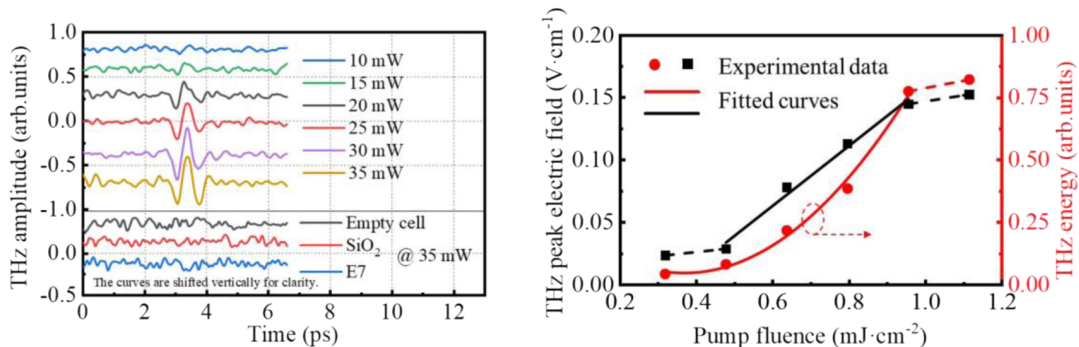


Fig. 3. (a) Normalized THz pulses with different pump powers. (b) THz peak electric field and energy from LC as a function of the pump fluence.

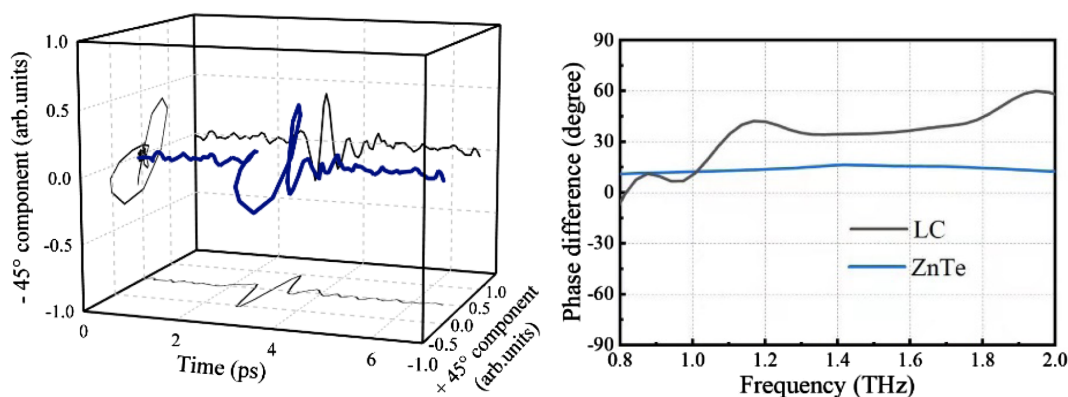


Fig. 4. (a) Three-dimensional trajectory plot of the temporal waveform of THz emission for $\theta = 45^\circ$. (b) Frequency-dependent phase difference calculated from the curves of 45° and -45° components presented in (a).

is low; therefore, it is difficult to increase the THz intensity by increasing the pump fluence. It would be worthwhile to further investigate this through phase matching, LC arrays, lenses, or spherical reflectors to enhance the THz emission intensity. There may be several possible mechanisms for the origin of the THz emission in addition to OR, such as the third-order nonlinear effect. Further experiments are necessary to fully understand the mechanism for the THz generation from LCs.

4. CONCLUSION

We reported the first observations of THz generation by a femtosecond laser in the LC NJU-LDn-4. The characteristics of THz radiation depend on the relative direction between pump polarization and LC orientation. The THz peak electric field varied linearly with pump power, which corresponds to traditional OR features. In addition, the unique properties of the THz radiation of elliptic polarization were demonstrated in this study. We believe that this is a common phenomenon in LCs with strong second-order nonlinear optical effects. Some ingenious methods of aligning LC molecules can induce larger second-order nonlinearity. The thickness of LCs can be easily controlled, and photo-alignment technology can be used for the director distribution of LCs in microscopic regions to realize phase matching. THz conversion efficiency and THz intensity are expected to be further improved with low loss and high stability LC materials. LCs are sensitive to external fields such as electric, magnetic, and optical fields; therefore, they can be used as a potential alternative to develop tunable THz sources with arbitrary polarization. Numerous potential applications are expected, not only in physics (for polarization-based imaging) and communication, but also in chemistry and biology for chiral molecules.

Funding. China Postdoctoral Science Foundation (2019M651768, 2020T130285); Natural Science Foundation of Jiangsu Province (BK20211277; Natural Science Foundation of Jiangsu Province, Major Project (BK20212004); Fundamental Research Funds for the Central Universities (021014380176, 021314380095).

Acknowledgment. We thank the National Laboratory of Solid State Microstructures for the use of its equipment.

Disclosures. The authors declare no conflicts of interest.

Data availability. Data underlying the results presented in this paper are not publicly available at this time but may be obtained from the authors upon reasonable request.

[†]These authors contributed equally to this work.

REFERENCES

1. B. Ferguson and X. C. Zhang, "Materials for terahertz science and technology," *Nat. Mater.* **1**, 26–33 (2002).
2. M. Tonouchi, "Cutting-edge terahertz technology," *Nat. Photonics* **1**, 97–105 (2007).
3. M. Hangyo, "Development and future prospects of terahertz technology," *Jpn. J. Appl. Phys.* **54**, 120101 (2015).
4. Y.-C. Shen, P. Upadhyaya, E. Linfield, and H. E. Beere, "Ultrabroadband terahertz radiation from low-temperature-grown GaAs photoconductive emitters," *Appl. Phys. Lett.* **83**, 3117–3119 (2003).
5. D. Cook and R. Hochstrasser, "Intense terahertz pulses by four-wave rectification in air," *Opt. Lett.* **25**, 1210–1212 (2000).
6. Q. Jin, E. Yiwen, K. Williams, J. Dai, and X.-C. Zhang, "Observation of broadband terahertz wave generation from liquid water," *Appl. Phys. Lett.* **111**, 071103 (2017).
7. T. Kampfrath, M. Battiato, P. Maldonado, G. Eilers, J. Nötzel, S. Mährlein, V. Zbarsky, F. Freimuth, Y. Mokrousov, S. Blügel, M. Wolf, I. Radu, and P. M. Oppeneer, "Terahertz spin current pulses controlled by magnetic heterostructures," *Nat. Nanotechnol.* **8**, 256–260 (2013).
8. H. Qiu, L. Zhou, C. Zhang, J. Wu, Y. Tian, S. Cheng, S. Mi, H. Zhao, Q. Zhang, D. Wu, B. Jin, J. Chen, and P. Wu, "Ultrafast spin current generated from an antiferromagnet," *Nat. Phys.* **17**, 388–394 (2021).
9. H. Zhao, X. Chen, C. Ouyang, H. Wang, D. Kong, P. Yang, B. Zhang, C. Wang, G. Wei, T. Nie, W. Zhao, J. Miao, Y. Li, L. Wang, and X. Wu, "Generation and manipulation of chiral terahertz waves in the three-dimensional topological insulator Bi_2Te_3 ," *Adv. Photon.* **2**, 066003 (2020).
10. F. Blanchard, L. Razzari, H. Bandulet, G. Sharma, R. Morandotti, J.-C. Kieffer, T. Ozaki, M. Reid, H. F. Tiedje, H. K. Haugen, and F. A. Hegmann, "Generation of 1.5 μJ single-cycle terahertz pulses by optical rectification from a large aperture ZnTe crystal," *Opt. Express* **15**, 13212–13220 (2007).
11. X. C. Zhang, X. F. Ma, and Y. Jin, "Terahertz optical rectification from a nonlinear organic crystal," *Appl. Phys. Lett.* **61**, 3080–3082 (1992).
12. T. O. Buchmann, E. J. R. Kelleher, K. J. Kaltenecker, B. Zhou, S.-H. Lee, O.-P. Kwon, M. Jazbinsek, F. Rotermund, and P. U. Jepsen, "MHz-repetition-rate, sub-mW, multi-octave THz wave generation in HMQ-TMS," *Opt. Express* **28**, 9631–9641 (2020).
13. C. Vicario, B. Monoszlai, M. Jazbinsek, S.-H. Lee, O.-P. Kwon, and C. P. Hauri, "Intense, carrier frequency and bandwidth tunable quasi single-cycle pulses from an organic emitter covering the terahertz frequency gap," *Sci. Rep.* **5**, 14394 (2015).

14. J. Hebling, A. G. Stepanov, G. Almási, B. Bartal, and J. Kuhl, "Tunable THz pulse generation by optical rectification of ultrashort laser pulses with tilted pulse front," *Appl. Phys. B* **78**, 593–599 (2004).
15. J. Hebling, K. L. Yeh, M. C. Hoffmann, B. Bartal, and K. A. Nelson, "Generation of high-power terahertz pulses by tilted-pulse-front excitation and their application possibilities," *J. Opt. Soc. Am. B* **25**, B6–B19 (2008).
16. P. G. de Gennes and J. Prost, *Physics of Liquid Crystals*, 2nd ed. (Clarendon/Oxford University, 1993).
17. Z. Shen, S. Zhou, X. Li, S. Ge, P. Chen, W. Hu, and Y. Lu, "Liquid crystal integrated metalens with tunable chromatic aberration," *Adv. Photon.* **2**, 036002 (2020).
18. L. Wang, X.-W. Lin, W. Hu, G.-H. Shao, P. Chen, L.-J. Liang, B.-B. Jin, P.-H. Wu, H. Qian, Y.-N. Lu, X. Liang, Z.-G. Zheng, and Y.-Q. Lu, "Broadband tunable liquid crystal terahertz waveplates driven with porous graphene electrodes," *Light Sci. Appl.* **4**, e253 (2015).
19. L. Wang, S. Ge, Z. Chen, W. Hu, and Y. Lu, "Bridging the terahertz near-field and far-field observations of liquid crystal based metamaterial absorbers," *Chin. Phys. B* **25**, 09422 (2016).
20. L. Wang, S. Ge, W. Hu, M. Nakajima, and Y.-Q. Lu, "Graphene-assisted high-efficiency liquid crystal tunable terahertz metamaterial absorber," *Opt. Express* **25**, 23873–23879 (2017).
21. A. V. Sukhov and R. V. Timashev, "Optically induced deviation from central symmetry; lattices of quadratic nonlinear susceptibility in a nematic liquid crystal," *JETP Lett.* **51**, 413–417 (1990).
22. I. C. Khoo and S. T. Wu, *Optics and Nonlinear Optics of Liquid Crystals* (World Scientific, 1993).
23. C. Dongzhong and Y. Xuehai, "Second-order nonlinear optical liquid crystalline polymers," *J. Polym. Mater. Sci. Eng.* **15**, 10–13 (1999).
24. L. Wang, X. W. Lin, X. Liang, J. B. Wu, W. Hu, Z.-G. Zheng, B.-B. Jin, Y.-Q. Qin, and Y.-Q. Lu, "Large birefringence liquid crystal material in terahertz range," *Opt. Mater. Express* **2**, 1314–1319 (2012).
25. J.-H. Jeong, B.-J. Kang, J.-S. Kim, M. Jazbinsek, S.-H. Lee, S.-C. Lee, I.-H. Baek, H. Yun, J. Kim, Y. S. Lee, J.-H. Lee, J.-H. Kim, F. Rotermund, and O.-P. Kwon, "High-power broadband organic THz generator," *Sci. Rep.* **3**, 3200 (2013).
26. F. Roeder, M. Shalaby, B. Beleites, F. Ronneberger, and A. Gopal, "THz generation by optical rectification of intense near-infrared pulses in organic crystal BNA," *Opt. Express* **28**, 36274–36285 (2020).
27. Q. Chen, M. Tani, Z. Jiang, and X.-C. Zhang, "Electro-optic transceivers for terahertz-wave applications," *J. Opt. Soc. Am. B* **18**, 823–831 (2001).
28. S. M. Harrel, R. L. Milot, J. M. Schleicher, and C. A. Schmuttenmaer, "Influence of free-carrier absorption on terahertz generation from ZnTe(110)," *J. Appl. Phys.* **107**, 033526 (2010).
29. V. A. Enikeeva, A. S. Zolot'ko, V. A. Makarov, I. A. Ozheredov, V. N. Ochkin, and A. P. Shkurinov, "Second harmonic generation by femtosecond in nematic liquid crystal," *Bull. Lebedev Phys. Inst.* **34**, 142–145 (2007).